World Conference on
Timber Engineering
Oslo 2023

SEISMIC ANALYSIS OF A MULTI-STORY TIMBER-CONCRETE BUILDING AND DESIGNING FOR REUSE

Sivert Lie[1], Themistoklis Tsalkatidis[2]

ABSTRACT: This research paper seeks to investigate the seismic performance of a hybrid timber-concrete building with multiple stories and explore the possibility of designing for reuse in low-seismicity regions. The building design incorporates hollow-core slabs (HCS) as flooring, a cross-laminated timber (CLT) panel core, and moment-resisting timber frames (MRTF). Various types of beam-to-column connections (BCC) from prior research are adopted in the MRTF. Modal response spectrum analysis of the building is conducted using the Eurocode 8 method, which takes into account the effect of connection ductility. The connections are assessed based on several factors, including story drift, on-site construction ease, disassembly ease, and the reuse potential for beams, columns, and connecting element. The advantages and disadvantages of the concept are discussed. The results show that a higher rotational stiffness in beam-to-column connections shifts the buildings first torsional mode to a higher mode and lower frequency, but generally lowers the reusability of the structural components.

KEYWORDS: Design for reuse, seismic design, disassemble, connections, sustainability, hollow-core slab

1 INTRODUCTION

The construction industry and the production of structural elements contributes to significant parts of the global carbon dioxide production [1]. The need for sustainable buildings that meet the demands from increasing population worldwide and limiting the increasing global temperature due to greenhouse gasses, requires structural engineers to adapt traditional methods of design into more environmentally friendly solutions. While being a large part of a building's mass [2], the use of innovative and emerging materials is generally considered harder for structural elements than for other parts of the building [3]. Recently, the concept of designing for reuse has been implemented in several projects with promising results.

Designing for future reuse increases the possibility of reusing structural elements in order to reduce the carbon footprint of a new building and the waste production from a demolished building. Combining sustainable materials like timber with reused concrete elements can be an important part of reducing the global climate emission from the construction industry, where the production of structural elements is responsible for a share of 15% [4]. The concrete production is a large part of this share due to the high number of concrete projects [5].

The yearly production of Hollow-core slabs (HCS) has been reported to reach 150 million cubic meters per year [6]. The concept of reusing HCS has only been implemented in niche projects until now, but a newly published standard NS 3682:2022 describes the process of demounting, documenting, and evaluation of the element quality [7]. Traditionally, HCS has been regarded as a diaphragm [8]. However, designing HCS with the goal of facilitating disassembly and reuse may necessitate the development of novel methods for interconnecting elements and for connecting to the supporting structure.

The concept of reusing timber elements has not been implemented in a large scale and it is relatively new. This is reported to be due to several factors, including the aging of timber, duration of load and load intensity. The general view, however, is that the bending strength and stiffness are not, or only marginally, affected by this, but investigation is difficult due to large natural variability of timber [9].

Timber-concrete buildings have been extensively investigated, and light-frame wood buildings have shown great resistance against earthquake, due to low mass [10] and ductility of nails [11]. When using engineering wood products in construction, such as glulam or Cross-laminated timber (CLT), the mechanisms for seismic energy dissipation are different than for steel or concrete buildings [12]. Seismic design of moment-resisting timber frames (MRTF) necessitates the incorporation of ductile failure in connections to enable energy dissipation, as timber exhibits brittle material characteristics. For structures located in low-seismicity regions, this approach can be combined with design for future reuse of structural components.

2 METHOD

The suggested method is based on a reference building, preliminary designed according to Eurocode 5 [13], using an ULS utilization ratio of approximately 70% for critical elements.

[1] Sivert Lie, Norwegian University of Life Sciences (NMBU), Norway, sivert.lie@nmbu.no
[2] Themistoklis Tsalkatidis, NMBU, themistoklis.tsalkatidis@nmbu.no

https://doi.org/10.52202/069179-0461

A numerical model of the building is modelled using SAP2000 [14], where beams and columns are modelled as frames with orthotropic material parameters. CLT is modelled as orthotropic thin shell with material property calculation according to [15]. HCS are modelled as thin shell with membrane thickness corresponding to the element height and bending thickness as 92% of the membrane thickness. To ignore the transverse bending stiffness, a modification factor is applied to reduce the transverse bending stiffness contribution to 1% of the longitudinal stiffness, creating a one-way slab. Table 1 shows the materials, the mass density of structural elements, and loads applied to the structure.

Table 1: *Weight and density of elements and applied loads.*

Element	Weight/Density
HCS 200 mm	271 kg/m^2
HCS 320 mm	425 kg/m^2
Glulam beam and columns	460 kg/m^3
CLT wall-panels (5-L, 200 mm)	440 kg/m^3
Additional dead load	1 kN/m^2
Snow load	2.8 kN/m^2
Live load	3.0 kN/m^2

2.1 REFERENCE BUILDING

The 8-floor reference building is shown in Figure 1. The central core consists of CLT-panels and the remaining bearing structure is glulam beams and columns, working as MRTF, with beam dimension of 480x765 mm^2. Column dimensions vary from 480x900 mm^2 for columns in grid A/F and E/F, and 480x720 mm^2 in grid B/C and D/C. HCS works as the separating floor. The top floor is +34 295 mm, and the general story height is 2.8 m. The first floor differs with a story height of 7 695 mm in grid A/F and E/F, and story height of 4980 mm in grid B/C and C/D. The global X- and Y-axis is parallel with gridline F4 and A1, respectively.

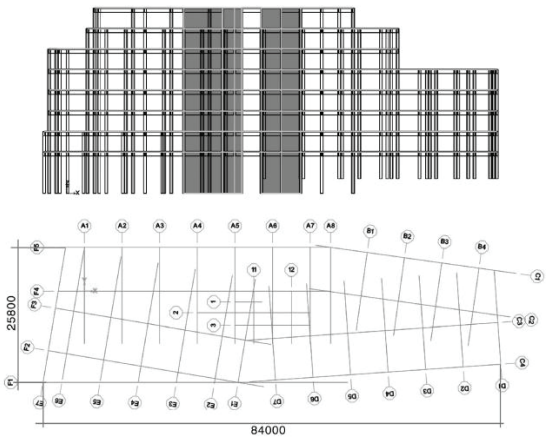

Figure 1: *Outline of reference building and grid.*

2.2 BEAM-TO-COLUMN CONNECTIONS

Several types of beam-to-column connections (BCC) from available research are implemented in the model. The connections are adjusted to fit the dimensions of the structural elements in the reference model, and all connections are based on continuous columns and intermediate beams. All connections are implemented in the analytical model as rotational springs at the beam ends. Two reference connections are made in order to investigate the effect of stiffness of the connections and get comparable extreme values. Pinned connection has springs with zero rotational stiffness, while the rigid connections are implemented with infinite rotational spring stiffness. The rotational stiffness K_R for each connection is based on the analytical formulation found in the respective research.

Following the results from experimental testing where the inclusion of lateral springs did not affect the results relatively much [16], lateral springs are set as rigid in all connections to get comparable results. Rotation of the connection about the column longitudinal axis is neglected as the HCS are assumed to prevent this motion.

Each connection is classified as either pinned, semi-rigid, or rigid according to EC3-1-8 [17], where the stiffness of a typical beam element is used. As the column distances are different in the two global directions, two classification values are used for X and Y, with beam length $L_{b,x}$ = 7200 mm and $L_{b,y}$ = 8400 mm, respectively.

2.2.1 Bolted connection

The determination of K_R for the bolted connection (BC) is based on traditional calculation methods described by EC5 with bolts and slotted steel plates [13]. Using the slip modulus of a single fastener K_{ser} and the corresponding radius from center of rotation r_i, the rotational stiffness in ULS is found using Equation (1):

$$K_R = \sum_{i=1}^{n} \left(2 \cdot \frac{2}{3} \cdot \frac{\rho_m^{1.5} \cdot d}{23} \right) \cdot r_i^2 \tag{1}$$

where ρ_m is the mean density of the connected element and d is the diameter of the bolt. The rotation point is assumed in the center of gravity of the bolts in the beam.

2.2.2 Top-and-seat steel angles connection

The top-and-seat steel angles connection (TS) is evolved from [18], using steel angles on both sides of the column for intermediate BCC connections. The calculation of the rotational stiffness K_R is based on formulation from [19, 20], and is seen in Equation (2):

$$K_R = \frac{h_b^2}{\frac{1}{K_{top}} + \frac{1}{K_{bot}}} \tag{2}$$

https://doi.org/10.52202/069179-0461

where h_b is the height of the beam. K_{top} depends on the bearing stiffness of the column face K_{cc}, axial stiffness of the bolt K_B and the tensile stiffness of the angle horizontal leg K_t. K_{bot} does not include the axial stiffness of the bolt as it is assumed that the bolt has no withdrawal stiffness. The springs are added as a series of springs. K_{CC} is expressed in Equation (3):

$$K_{CC} = \frac{E_{90}\, b_c\, l_{eff,cc}}{h_c} \tag{3}$$

where E_{90} is the modulus of elasticity perpendicular to grain, b_c is the width of the column, $l_{eff,cc}$ is the effective length of the area in compression and h_c is the depth of the column [21]. K_B is expressed in Equation (4) according to [22], using the modulus of elasticity for steel E_s, the cross-sectional area of the bolt A_b and the effective length of the bolt L_b. n is the number of bolts considered to contribute to K_R.

$$K_B = \frac{A_b\, E_s}{L_b} \cdot n \tag{4}$$

K_t is found using the steel angle dimensions and the distance from the critical yielding point to the vertical bolt [22], as seen in Equation (5):

$$K_t = \frac{E \cdot p \cdot t}{a'} \tag{5}$$

2.2.3 Glued-in steel rods connection

The calculation of K_R for the glued-in steel rods connection (GIR) is found using the tensile stiffness of glued-in rods for the tensile stiffness K_{tens} of the connection. The compressive stiffness K_{comp} of the connection is found adding a series of springs where the shear stiffness of the column K_{CS} is expressed by [21], the transverse stiffness of the column K_{CC} as in Equation (3) and the stiffness of the glulam beam in compression K_{BC} defined by [23]. Based on an adapted version from [21], an equation for the rotational stiffness is shown in Equation (6):

$$K_R = \frac{z_{eq}^2}{\frac{1}{K_{tens}} + \frac{1}{K_{comp}}} \tag{6}$$

Where z_{eq} is the equivalent lever arm between the tensile and compressive resultant. K_{tens} is found using the effective stiffness of a rod row and the distance from the bolt row to the center of compression [21]. The design of this connection leads to the connections showing great ductility in experimental testing [24].

2.2.4 Inclined threaded rods connection

The inclined threaded rods connection (ITR) is adopted from [25] and consist of screwed in rods in both the column and beam. The rods are fastened with steel rings, and the rings work as load transferring between the beam and column.

The calculation of K_R is based on component-method, where the stiffness contribution at the column side $K_{ax.c}$ is found using the axial stiffness $K_{ax,l0}$ and the withdrawal stiffness $K_{ser,ax}$ of the rods. Compliance terms S_{xx} and S_{xy} are used to consider the angle of rods. By converting from at point load to a uniformly distributed load acting on a clamped beam, the expression for the stiffness contribution at the column side $K_{R,C}$ is expressed in Equation (7):

$$K_{R,C} = \frac{h_b^2}{\left(S_{xx,c}^{c_1-c_2} + S_{xx,c}^{c_3-c_4}\right) + \left(S_{xy,c}^{c_3-c_4} - S_{xy,c}^{c_1-c_2}\right) \cdot \frac{3h_b}{L_b}} \tag{7}$$

For the stiffness at the beam side $K_{R.B}$, the lateral stiffness K_v of the rod is included in the compliance terms to consider the global direction of the rods:

$$K_{R,B} = \frac{h_b^2}{\left(S_{xx,b1} + S_{xx,b2}\right) + \left(S_{xy,b2} - S_{xy,b1}\right) \cdot \frac{3h_b}{L_b}} \tag{8}$$

The stiffness contribution from the steel rings $K_{R,con}$ is found through numerical analysis and provides 484 kN/mm and 600 kN/mm in compression and tension, respectively [25]. This leads to the equation for K_R seen in Equation (9):

$$K_R = \left(\frac{1}{K_{R,C}} + \frac{1}{K_{R,B}} + \frac{1}{K_{R,con}}\right)^{-1} \tag{9}$$

2.2.5 Overview of rotational stiffness

By applying the dimensions of the structural elements described in 2.1, where some of the connections depend more on the orientation and dimensions of the column, the rotational stiffness for each connection is presented in Table 2. Notation 1 indicates connections located at grid A/F or E/F, while notation 2 refers to grid B/C and C/D, see Figure 1. For the TS, GIR and ITR, four planes of rods are used, and for the bolted connection 16 M16 bolts are placed in a rectangular formation.

Table 2: *Calculated rotational stiffness of investigated connections.*

Connection	Global direction	K_R [kNm/rad]	Rigidity-class
Pinned		0	Pinned
Rigid		∞	Rigid
Bolted		5 629	Pinned
Top-and-seat steel angles	X Y_1 Y_2	49 961 26 684 30 191	Semi-rigid
Glued-in steel rods	X_1 X_2 Y_1 Y_2	53 481 33 938 50 741 38 669	Semi-rigid
Inclined threaded rods	X Y_1 Y_2	51 606 58 705 54 970	Semi-rigid

2.3 CONNECTION HOLLOW-CORE SLABS

The slab consisting of HCS is assumed as a diaphragm with rigid interconnections in the numerical analysis. The connection between HCS to timber beams is based on the connection of a timber-concrete-composite from [26], using vertical glued-in rods glued in the glulam beam and casted together with the HCS. This connection is implemented as a hinged connection in the numerical analysis.

2.4 MODAL RESPONSE SPECTRUM ANALYSIS

Modal response spectrum analysis (MRSA) is done according to EC8 [27] for each connection case, where the value for peak ground acceleration (PGA) is assumed for a building located in Oslo, Norway. This leads to a ground acceleration of reference ground acceleration of 0.3 m/s^2.

As the building is vulnerable for torsional effects, the Complete Quadratic Combination (CQC)-method proposed by EC8 is used for combination of modes. The seismic effect in the global directions X and Y is combined by adding 30% of the seismic effect from one direction to the other.

For a building in seismic class IIIa and ground type D, the parameters Type 2 design response spectrum is shown in Table 3. The average joint absolute drift for each connection case is found. A behavior factor of q = 1.5 is used for the design spectrum for all connection cases except GIR, where q = 2.5.

Table 3: *Parameters for creating Type 2 elastic spectrum.*

Ground type	S	T_B [s]	T_C [s]	T_D [s]
D	1.8	0.1	0.3	1.2

3 CONNECTION EVALUATION

The results from the analysis show that less rigid connections lead to a torsional mode being present at a lower frequency. Increasing the rigidity of the BCC leads to torsional modes being present at higher frequency and less participating modes. The comparison of results from the MRSA for each BCC indicates that increasing the rotational stiffness increases the absolute- and interstory drift.

3.1 PINNED CONNECTION

For the pinned connection, the modes and corresponding contributing mass are listed in Table 4. The first mode is a torsional mode, and the cumulative mass participation ratio exceed 90% in mode 6.

Table 4: *Modes and participation ratio for pinned connection.*

Mode	Period [s]	m_X [%]	m_Y [%]	m_{RZ} [%]
1	2.81	0.1	0.0	70.4
2	1.442	1.1	76.4	0.0
3	1.286	78.2	1,1	0.1
4	0.794	0.1	0.0	17.5
5	0.415	12.1	1.4	0.0
6	0.403	1.5	12.5	0.1
	∑	**93.5**	**91.4**	**88.3**

For the MRSA of the pinned connection, the average story displacement is shown in Figure 2, with a maximum drift of 30.7 mm at the top story. The maximum interstory drift of 5.5 mm is found in story 1 with seismic loading in global Y as the dominant load.

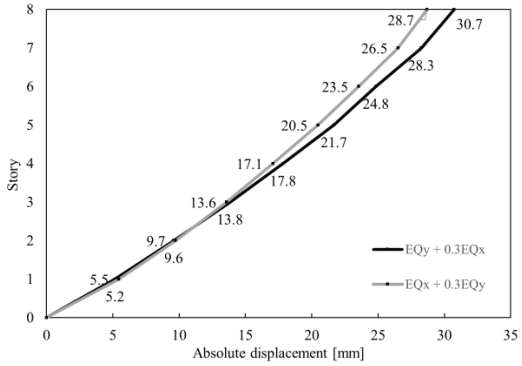

Figure 2: *Average story displacement for pinned connection.*

3.2 RIGID CONNECTION

For the rigid connection, the modes and corresponding mass participation ratios are listed in Table 5. The first torsional mode occurs at mode 3 and the cumulative mass participation ratio exceeds 90% in mode 5.

https://doi.org/10.52202/069179-0461

Table 5: *Modes and participation ratio for rigid connection.*

Mode	Period [s]	m_X [%]	m_Y [%]	m_{RZ} [%]
1	1.184	21.2	64.4	1.3
2	1.065	59.1	23.1	4.3
3	1.003	4.7	0.0	81.7
4	0.349	2.3	6.2	0.0
5	0.318	7.0	2.0	0.0
	∑	**94.3**	**95.7**	**87.3**

For the MRSA of the rigid connection, the average joint absolute drift is shown in Figure 3, with maximum drift of 46.7 mm at the top story. The maximum interstory drift of 14.4 mm is found in story one with the seismic loading in global X as the dominant load.

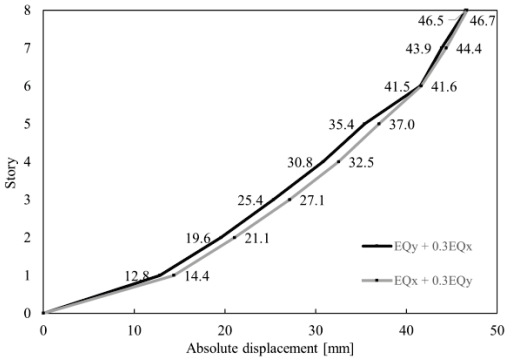

Figure 3: *Average story displacement for rigid connection.*

3.3 BOLTED CONNECTION

For BC, the modes and corresponding contributing mass are listed in Table 6. The first mode is a torsional mode, and the cumulative mass participation ratio exceed 90% in mode 6.

Table 6: *Modes and participation ratio for BC.*

Mode	Period [s]	m_X [%]	m_Y [%]	m_{RZ} [%]
1	2.407	0.1	3.0	72.1
2	1.401	0.0	75.5	2.3
3	1.245	80.6	0.0	0.1
4	0.734	0.1	0.0	14.6
5	0.409	2.9	10.1	0.0
6	0.387	9.6	3.1	0.1
	∑	**93.3**	**91.7**	**89.2**

For the MRSA of BC, the average story displacement is shown in Figure 4, with a maximum drift of 25.9 mm at the top story. The maximum interstory drift of 5.4 mm is found in story 1 with seismic loading in global X as the dominant load.

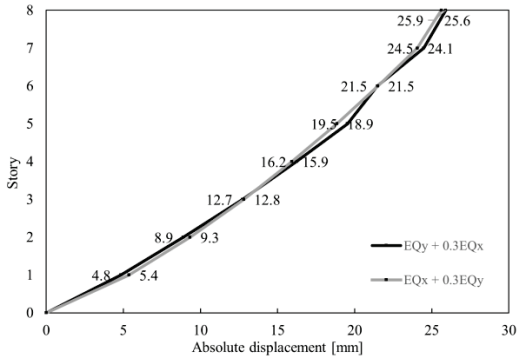

Figure 4: *Average story displacement for BC.*

3.4 TOP-AND-SEAT STEEL ANGLE CONNECTION

For TS the modes and corresponding contributing mass are listed in Table 7. The first torsional mode occurs at mode 3, and the cumulative mass participation ratio exceed 90% in mode 6.

Table 7: *Modes and participation ratio for TS.*

Mode	Period [s]	m_X [%]	m_Y [%]	m_{RZ} [%]
1	1.303	0.0	68.2	13.2
2	1.126	81.8	0.2	2.2
3	1.121	2.3	12.2	65.2
4	0.394	0.1	10.5	1.4
5	0.344	0.1	1.2	9.4
6	0.340	10.2	0.1	0.1
	∑	**94.5**	**92.4**	**91.5**

For the MRSA of TS, the average story displacement is shown in Figure 5, with a maximum drift of 23.6 mm at the top story. The maximum interstory drift of 6.1 mm is found in story 1 with seismic loading in global X as the dominant load.

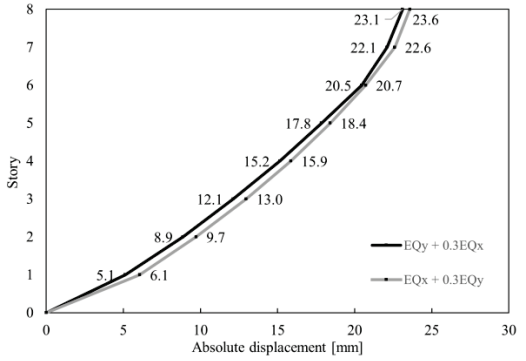

Figure 5: *Average story displacement for TS.*

https://doi.org/10.52202/069179-0461

3.5 GLUED-IN STEEL RODS CONNECTION

For GIR, the modes and corresponding contributing mass are listed in Table 8. The first torsional mode occurs at mode 3, and the cumulative mass participation ratio exceed 90% in mode 6.

Table 8: *Modes and participation ratio for GIR.*

Mode	Period [s]	m_X [%]	m_Y [%]	m_{RZ} [%]
1	1.283	0.2	69.8	11.9
2	1.122	83.8	0.0	0.6
3	1.110	0.4	11.2	68.8
4	0.391	0.2	10.8	0.8
5	0.340	0.4	0.7	0.8
6	0.332	9.7	0.1	9.3
	∑	**94.6**	**92.6**	**91.7**

For the MRSA of GIR, the average story displacement is shown in Figure 6, with a maximum drift of 16.7 mm at the top story. The maximum interstory drift of 3.9 mm is found in story 1 with seismic loading in global X as the dominant load.

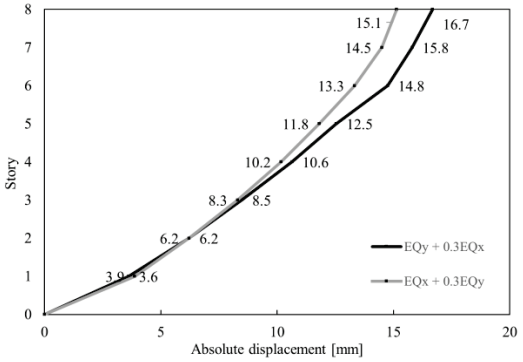

Figure 6: *Average story displacement for GIR.*

3.6 INCLINED THREADED RODS CONNECTION

For ITR the modes and corresponding contributing mass are listed in Table 9. The first torsional mode occurs at mode 3, and the cumulative mass participation ratio exceed 90% in mode 5.

Table 9: *Modes and participation ratio for ITR.*

Mode	Period [s]	m_X [%]	m_Y [%]	m_{RZ} [%]
1	1.246	3.6	71.4	7.6
2	1.120	80.7	3.0	0.7
3	1.092	0.0	7.4	74.1
4	0.384	2.3	8.6	0.1
5	0.339	7.6	2.5	0.4
	∑	**94.2**	**92.9**	**82.9**

For the MRSA of the inclined threaded rods connection, the average story displacement is shown in Figure 7, with a maximum drift of 24.6 mm at the top story. The maximum interstory drift of 6.3 mm is found in story 1 with seismic loading in global X as the dominant load.

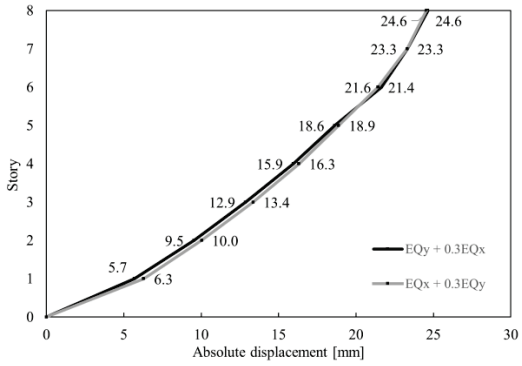

Figure 7: *Average story displacement for ITR.*

4 DISCUSSION

In addition to the numerical results presented, each BCC is discussed based on several parameters: ease of construction on-site, ease of disassembly, reuse potential of beams, columns and connecting elements and aesthetics of connection.

4.1 STRUCTURAL BEHAVIOR

The absolute displacements from the MRSA are calculated using the average joint displacements in each floor. For connection cases where two torsional modes are present before the cumulative mass participation ratio exceeds 90%, the internal variation in joint displacement is higher than connections with only one torsional mode.

By comparing the result from the MRSA with E_Y as the dominant seismic load, Table 10 shows that the tendency is that connections that offer lower rotational stiffness has the first torsional mode outside of the spectrum where the pseudo-acceleration is significant.

For a building in an area with low value for ground acceleration, this means that a connection with low rotational stiffness can be a better option with regards to seismic performance.

Table 10: *Comparison of first torsional mode, torsional mass participation ratio, and the corresponding pseudo-acceleration.*

Connection	T [s]	m_{RZ} [%]	a_g [g]
Pinned	2.810	70.4	0.008
Rigid	1.003	81.7	0.034
BC	2.407	72.1	0.008
TS	1.121	65.2	0.031
GIR	1.110	81.2	0.019
ITR	1.092	74.1	0.032

https://doi.org/10.52202/069179-0461

4.2 EASE OF CONSTRUCTION ON-SITE

The ease of construction on-site is critical for efficient construction process of a building. BCC with an extensive process with necessary high precision is time consuming and harder to construct on-site.

ITR is rather comprehensive to construct and require high precision to acquire the rotational stiffness from the numerical formulation. The effect of different rod-to-grain angle than used to calculate the rotational stiffness affects the rotational stiffness significantly [25]. Following this, the insertion of rods in both the beam and the column should be done in a controlled environment (typically off-site) and leads to low on-site flexibility.

The same applies to GIR because contact between the beam and column faces is critical. This is due to the spring stiffness of the column face, K_{cc}, which is one of the decisive parameters for the rotational stiffness. As a result, the mounting process is time-consuming and has minimal tolerance for errors both in production and during assembly. However, if the on-site margin of error is within the tolerance limits and the necessary off-site preparations are completed, the assembly process may be time-effective.

4.3 EASE OF DISASSEMBLY

The ease of disassembly is critical for efficient tear-down of buildings and possibility for reusing structural elements. Connections with more permanent connecting elements, typically glue or welds, are considered having lower reuse potential [28] and a relatively low reversibility [29].

This leads to GIR being a less suitable alternative when considering possibilities for future reuse of beams and columns. The structural performance of this connection depends on the withdrawal capacity of glued-in rods, making the reversibility of the connection, without causing damage to the column, beam, or rods, low.

Conversely, connections that utilize bolts and screws as connecting elements require less time for disassembly [29]. This implies that the traditional bolted connection, the steel angle connection, and the inclined threaded rods connection may all be relatively easy to disassemble.

4.4 REUSE POTENTIAL OF BEAMS, COLUMNS AND CONNECTING ELEMENTS

The reuse potential for the components in each BCC is discussed, where the potential is based on the possible failure mode of the BCC, and the affected area of the beam and column. The reuse of connected and connecting elements is based on the possibility of reusing components of the connection. Connections with more permanent connecting elements, typically glue or welds, are considered having lower reuse potential [28].

One issue with the traditional type of timber connections, like BC, can be residual displacement caused by non-linear behavior of the timber under initial load. This happens due to imperfections in the timber surface facing the connector and occurs even if the dowels are tightly fitted [30]. This means elements involving bolts should be checked for damages, and most probably the portion of the elements with bolt holes should be deposited. Bolted connections should also generally be designed for ductile failure of the connector [13] and due to this requirement, the bolts should not be reused for structural purpose. The possibility of removing the affected portion of the beam and column is incidentally the cased for all connections discussed, but especially relevant for GIR, as the rods are time-consuming to remove.

ITR can have the highest potential for reuse, but this requires designing the next project based on the available beams and columns. This concept is referred to as stock-constrained design [31].

4.5 REUSE OF HOLLOW-CORE SLABS

To include HCS in the design of a sustainable building, the design process should evaluate if the building is going to be designed using an existing stock of materials, designed for future reuse. The optimal solution would be to combine these two concepts, but as for HCS, the concept of including already existing elements seems to be the better option. The reasoning behind this is the large amount of already produced HCS.

The HCS should be connected to the timber beams using the same concept as for glued in shear studs, creating a timber-concrete composite. This is shown to reach good shear capacity [26] and can also be utilized to reduce the necessary cross-sectional area of the timber beams due to timber-concrete-composite effect.

4.6 EVALUATION OF THE CONCEPT

The advantages with the concept of reusing and designing for future reuse is described to be of significant value. Utilization of already produced structural elements introduce a potential of reducing significant amounts of global greenhouse gas emissions. The disadvantages are, on the other hand, what significantly raises the threshold to fully utilize the potential reduction of environmental burden the construction of a new building.

For structural elements, the process of tearing down a building often implies rough treatment for vulnerable elements like timber. To facilitate future reuse of these elements, the process needs to be changed from demolition to disassembling. The integration of disassembling will increase the time consumption of tearing down a building significantly and consequently increasing the cost.

To implement connections with higher rotational stiffness more suitable for modular buildings, the concept of stock-

constrained design may be an effective method to utilize already produced elements. However, when using this method, the design of the new building is restricted by available materials. This could lead to a lower utilization of available land area, and implicit meaning a higher cost per area.

5 CONCLUSION

In this paper a modal response spectrum analysis according to EC8 is done for a reference building consisting of a variety of beam-to-column connection from available research, hollow-core slabs as separating floor and a CLT-core.

The results of the presented study show that a higher rotational stiffness in beam-to-column connections shifts the buildings first torsional mode to a higher mode and lower frequency, but generally lowers the reusability of the structural components. Therefore, in the cases where the reusability is prioritized, the evaluated connections with higher rotational stiffness beam-to-column connections may not be the best alternative. However, according to the findings of the numerical investigation, it is possible to combine design for seismic loadings in low-seismicity regions with designing for future reuse by selecting beam-to-column connections with appropriate characteristics. Overall, this is a promising option for the design of future projects.

REFERENCES

[1] Ghayeb H. H., Razak H. A., Sulong N. H. R.: Evaluation of the CO2 emissions of an innovative composite precast concrete structure building frame. *J Clean Prod*, 242:118567, 2020.

[2] Eberhardt C. L. M., Birgisdóttir H., Birkved M.: Life cycle assessment of a Danish office building designed for disassembly, 2018.

[3] Peretti G., Druhmann C. K., Bleiziffer S., Brown J., Campama Pizarro M., del Río Merino R., *et al.*: Working Group Three Report: Regenerative Construction and Operation. *RESTORE - REthinking Sustainability TOwards Regenerative Economy*, 2019.

[4] Joensuu T., Leino R., Heinonen J., Saari A.: Developing Buildings' Life Cycle Assessment in Circular Economy-Comparing methods for assessing carbon footprint of reusable components. *Sustain Cities Soc*, 77:103499, 2022.

[5] Adesina A.: Recent advances in the concrete industry to reduce its carbon dioxide emissions. *Environmental Challenges*, 1, 2020.

[6] de Castilho V. C., Nicoletti M. do C., el Debs M. K.: An investigation of the use of three selection-based genetic algorithm families when minimizing the production cost of hollow core slabs. *Comput Methods Appl Mech Eng*, 194(45–47):4651–4667, 2005.

[7] Standard Norge: NS 3682:2022 Hulldekker av betong til ombruk, 2022.

[8] Memari A., Ramaji I. J.: Identification of structural issues in design and construction of multi-story modular buildings, 2013.

[9] Niu Y., Rasi K., Hughes M., Halme M., Fink G.: Prolonging life cycles of construction materials and combating climate change by cascading: The case of reusing timber in Finland. *Resour Conserv Recycl*, 170, 2021.

[10] Bağbanci M. B., Bağbanci Ö. K.: The Dynamic Properties of Historic Timber-Framed Masonry Structures in Bursa, Turkey. *Shock and Vibration*, 2018.

[11] Pan Y., Tannert T., Kaushik K., Xiong H., Ventura C. E.: Seismic performance of a proposed wood-concrete hybrid system for high-rise buildings. *Eng Struct*, 238:112194, 2021.

[12] Gallo P. Q., Carradine D. M., Ramiro Bazaez ·.: State of the art and practice of seismic-resistant hybrid timber structures. *European Journal of Wood and Wood Products*, 79:5–28, 2021.

[13] EN 1995-1-1: Eurocode 5: Design of timber structures - Part 1-1: General - Common rules and rules for buildings. Standard Norge, NS-EN 1995-1-1:2004+A1:2008+NA:2010 2004.

[14] CSI America.: SAP2000, 2021.

[15] Follesa M., Christovasilis I. P., Vassallo D., Fragiacomo M., Ceccotti A.: Seismic design of multi-storey cross laminated timber buildings according to Eurocode 8. *Ingegneria Sismica*, 4, 2013.

[16] Vilguts A., Stamatopoulos H., Malo K. A.: Parametric analyses and feasibility study of moment-resisting timber frames under service load. *Eng Struct*, 228:111583, 2021.

[17] EN 1993-1-8: Eurocode 3: Design of steel structures - Part 1-8: Design of joints. NS-EN 1993-1-8:2005+NA:2009, 2005.

[18] Zhou S. R., Li Z. Y., Feng S. Y., Zhu H., Kang S. B.: Effects of bolted connections on behaviour of timber frames under combined vertical and lateral loads. *Constr Build Mater*, 293:123542, 2021.

[19] Tsalkatidis T., Amara Y., Embaye S., Nathan E.: Numerical investigation of bolted hybrid steel-timber connections. *Front Built Environ*, 4, 2018.

[20] Karagiannis V., Málaga-Chuquitaype C., Elghazouli A. Y.: Behaviour of hybrid timber beam-to-tubular steel column moment connections. *Eng Struct*, 131:243–263, 2017.

[21] Yang H., Liu W., Ren X.: A component method for moment-resistant glulam beam–column connections with glued-in steel rods. *Eng Struct*, 115:42–54, 2016.

[22] Málaga-Chuquitaype C., Elghazouli A. Y.: Component-based mechanical models for blind-bolted angle connections. *Eng Struct*, 32(10):3048–3067, 2010.

https://doi.org/10.52202/069179-0461

[23] Tomasi R., Zandonini R., Piazza M., Andreolli M.: Ductile End Connections for Glulam Beams. *Structural Engineering International*, 18:290–296, 2008.
[24] Fairweather R. H.: Beam Column Connections for Multi-storey Timber Buildings A Report, 1992.
[25] Stamatopoulos H., Malo K. A., Vilguts A.: Moment-resisting beam-to-column timber connections with inclined threaded rods: Structural concept and analysis by use of the component method. *Constr Build Mater*, 322:126481, 2022.
[26] Ling Z., Zhang H., Mu Q., Xiang Z., Zhang L., Zheng W.: Shear performance of assembled shear connectors for timber–concrete composite beams. *Constr Build Mater*, 329:127158, 2022.
[27] EN 1998-1: Eurocode 8: Design of structures for earthquake resistance - Part 1: General rules, seismic actions and rules for buildings. NS-EN 1998-1:2004+A1:2013+NA:2021, 2004.
[28] Hradil P.: Barriers and opportunities of structural elements re-use, 2014.
[29] Kondo Y., Deguchi K., Hayashi Y. I., Obata F.: Reversibility and disassembly time of part connection. *Resour Conserv Recycl*, 38(3):175–184, 2003.
[30] Reynolds T., Harris R., Chang W.-S.: In-service dynamic stiffness of dowel-type connections, 2013.
[31] Warmuth J., Brütting J., Fivet C.: Computational Tool for Stock-Constrained Design of Structures, 2021.